

## RESEARCH

# Sensitivities of Normalized Difference Vegetation Index and a Green/Red Ratio Index to Cotton Ground Cover Fraction

G. L. Ritchie,\* D. G. Sullivan, W. K. Vencill, C. W. Bednarz, and J. E. Hook

## ABSTRACT

Vegetation indices based solely on visible reflectance may simplify and decrease the cost of crop growth estimates compared to visible and near-infrared (NIR) indices. Ground-based and aerial visible and visible/NIR vegetation indices based on aerial images were compared for sensitivity to ground cover fraction (GCF) of cotton (*Gossypium hirsutum* L.) under four irrigation treatments in 2004 and five treatments in 2005 and 2006. In-season cotton imagery was collected using an unmodified Nikon COOLPIX 4300 camera and a COOLPIX 4300 camera modified for NIR imaging attached to a tethered blimp. GCF imagery was collected at 45 to 60 m and compared with normalized difference vegetation index (NDVI) and green/red ratio values from imagery collected at 180 to 250 m. Ground-based (1.5 m) spectrometer NDVI measurements using multiple spectral regions were also evaluated. Spectrometer ( $r^2 = 0.40$  to  $0.80$ ) and camera ( $r^2 = 0.68$  to  $0.90$ ) indices were highly correlated with season-wide GCF between fractions of 0.20 and 0.80 and were sensitive to irrigation treatments. Camera green/red ratio was linearly correlated with GCF throughout the 3 yr. The pooled comparison for the 3 yr was strongly linear ( $r^2 = 0.86$ ). Our results suggest that the green/red ratio index might allow quick, simple, and accurate crop growth estimates for production.

G.L. Ritchie and J.E. Hook, Univ. of Georgia, 2356 Rainwater Rd., P.O. Box 748, Tifton, GA 31793-0748. D.G. Sullivan, TurfScout, LLC, Tifton, GA 31794. W.K. Vencill, 4103 Miller Plant Sciences Bldg., Univ. of Georgia, Athens, GA 30602. C.W. Bednarz, Texas Tech Univ. and Texas AgriLife Research, Box 42122, Lubbock, TX 79409. Received 15 Apr. 2009. \*Corresponding author (gritchie@uga.edu).

**Abbreviations:** GCF, ground cover fraction; NDVI, normalized difference vegetation index; NIR, near-infrared.

REMOTE SENSING offers a practical solution to the need for large-scale plant growth and health estimates. Current remote sensing platforms such as satellites, airplanes, and ground-based platforms can be used to obtain field-scale imagery (Sui et al., 2005; Vierling et al., 2006; Yang et al., 2001, 2003) and offer an alternative to intensive soil or tissue sampling for broad-scale crop growth and health estimates (Hatfield et al., 2008). Ground cover fraction (the fraction of an area of interest within an image covered by vegetative biomass) estimates and remote sensing vegetation indices can identify plant growth and aid in management decisions (Booth et al., 2006, 2008, and others). Indices that require only a single camera and minimal processing can save time and money in image analysis.

## Ground Cover Fraction and Crop Growth

The GCF has been used to estimate crop growth and as a baseline for other remote sensing measurements (Boissard et al., 1992; Chen and Vierling, 2006; Klassen et al., 2003), because it is closely related to crop growth and radiation capture (Asrar et al., 1992). The GCF measurements are commonly made at a nadir viewing angle (Purevdorj et al., 1998). The images are processed digitally, and plant pixels are separated from soil pixels in software, either

Published in Crop Sci. 50:1000–1010 (2010).

doi: 10.2135/cropsci2009.04.0203

Published online 10 Mar. 2010.

© Crop Science Society of America | 5585 Guilford Rd., Madison, WI 53711 USA

All rights reserved. No part of this periodical may be reproduced or transmitted in any form or by any means, electronic or mechanical, including photocopying, recording, or any information storage and retrieval system, without permission in writing from the publisher. Permission for printing and for reprinting the material contained herein has been obtained by the publisher.

manually or using software that has been designed to discriminate between image features such as plants, soil, rocks, and shadows (Booth et al., 2006). Ground cover measurements have the potential to be very precise estimators of crop growth, because images taken close to the crop canopy under favorable lighting conditions discriminate precisely between plants and the background (Klassen et al., 2003).

The limiting factor for GCF measurements under ideal conditions is not precision, but the time and expertise needed to perform the analysis. Even when automatic machine processing is available, the proper field of view must be extracted and aligned. As the distance between the camera and plants increases, spatial resolution becomes an issue (Calera et al., 2001). At low spatial resolution, pixel separation and classification become difficult, and vegetation indices become the preferred method of image analysis. Overhead imagery can be used to calculate both GCF and vegetation indices, but conditions that lend themselves to accurate ground cover estimates include lack of shadows and high ground resolution, whereas spectral vegetation indices benefit from sunny days and are not as sensitive to ground resolution.

## Vegetation Indices

Remote sensing vegetation indices determine crop growth and color by measuring reflected shortwave radiation. One vegetation index class uses ratios or normalized ratios of reflected visible and NIR radiation to improve sensitivity to crop growth (Bannari et al., 1995; Elvidge and Chen, 1995). These indices capitalize on spectral differences between plants and soils, thereby minimizing differences in soil background reflectance, solar irradiance, and atmospheric effects (Elvidge and Chen, 1995; Huete, 1988; Rouse et al., 1973). Plants have low red and blue reflectance, low to intermediate green reflectance, and high NIR reflectance. Soil reflectance tends to be flat with a slight upward slope throughout the visible and NIR.

Combinations of green, red, red edge, and NIR reflectance have been consistently well correlated with crop growth and health, due to chlorophyll absorbance of visible radiation and the high NIR reflectance of leaves (Carter and Spiering, 2002; Gitelson and Merzlyak, 1998; Horler et al., 1983b). Vegetative indices are also well correlated with crop GCF. If soil, plant, and atmospheric effects are accounted for, these vegetation indices provide a robust method to identify crop growth characteristics and detect general stress events (Osborne et al., 2002; Pinter et al., 2003; Plant et al., 2000). Reduced costs and improvements in timeliness will continue to expand the use of remote sensing technology.

One commonly used vegetation index is the NDVI, with variants that are used to correct for soil or atmospheric effects (Huete, 1988; Huete et al., 1985; Plant et al., 2000; Rouse et al., 1973). The NDVI consists of a ratio of reflectance at two wavelengths ( $\lambda_1$ ,  $\lambda_2$ ) in the form  $(\lambda_1 - \lambda_2) / (\lambda_1 + \lambda_2)$ . Alternatively, this index can be calculated using broad

visible and NIR spectral regions. The reference wavelength ( $\lambda_r$ ) is often in the NIR portion of the spectrum, since chlorophyll does not absorb NIR radiation (Curran, 1989). The most common version of the NDVI uses a combination of red and NIR reflectance (Rouse et al., 1973), but other ratios have been shown to have a more linear correlation with GCF and crop chlorophyll content (Gitelson and Merzlyak, 1997; Ritchie and Bednarz, 2005).

Although narrow-band indices from hyperspectral sensors offer wavelength selectivity that is unavailable with broad band indices, research has shown that broad band indices can provide comparable measurements of vegetation quantity (Broge and Leblanc, 2001; Elvidge and Chen, 1995; Thenkabail et al., 2002). Broad band indices allow the use of cameras for remote sensing, and advancements in resolution and sensitivity may allow the use of low-cost, lightweight cameras instead of bulky, research grade instruments.

Reflected radiation can be measured with a simple three-channel RGB camera, such as off-the-shelf consumer models. These cameras are widely available and user friendly, and many of them have features that allow manual adjustments of shutter speed, white balance, and sensitivity, as well as logging of camera settings. Measuring NIR reflectance requires a camera with filters that block incoming visible light and transmit incoming NIR radiation (Ritchie et al., 2008). This requires either an in-camera filter mosaic that includes NIR filters and a four-channel output, or a separate optical system that measures NIR radiation. Four channel visible-NIR consumer cameras are not currently marketed, and combining separate RGB and NIR images requires image to image registration using specialized software. The silicon photodiodes used in visible optical systems are insensitive to IR radiation above about 1000 nm (ASD, 1999), so mid-infrared measurements are beyond the capabilities of consumer digital cameras. A simple visible vegetation index, such as the green/red ratio described by Adamsen et al. (1999), can be simpler and save money compared to indices that use visible and NIR reflectance, since the index relies only on visible reflectance. Classical studies have shown the green/red ratio to be highly related to green plant growth and biomass (Kanemasu, 1974; Tucker, 1979).

Remote sensing of plant stress for in-season management decisions such as irrigation might benefit from a simple visible imaging technique, because dynamic crop growth characteristics require rapid processing. In-season analysis must be quick, simple, and sensitive enough to changes in vegetative growth to let the producer make irrigation and other decisions. Minimizing the costs and processing time is a vital component of successful in-season remote sensing, since management decisions require data that is available and useful. The simplification of a remote sensing system can also make it practical for more frequent measurements during a production season.

**Table 1. Tillage, irrigation treatments, and plot design for 2004–2006.**

	2004	2005	2006 (strip)	2006 (conventional)
Tillage	Strip	Conventional	Strip	Conventional
Irrigation system	Variable rate center pivot	Lateral move system with on/off switches	Lateral move system with on/off switches	Lateral move system with on/off switches
Number of plots	16	20	20	16
Number of replicates	4	4	4	4
Irrigation treatments	na <sup>†</sup> 40-kPa Watermark trigger <sup>‡</sup> Aerial trigger <sup>§</sup> Aerial trigger–3 d <sup>¶</sup> Nonirrigated	20-kPa Watermark trigger 40-kPa Watermark trigger Aerial trigger Aerial trigger–3 d Nonirrigated	20-kPa Watermark trigger 40-kPa Watermark trigger Aerial trigger Aerial trigger–3 d Nonirrigated	20-kPa Watermark trigger 40-kPa Watermark trigger Aerial trigger Aerial trigger–3 d na
Plot design	Latin square	Randomized complete block	2 Factor randomized block	2 Factor randomized block

<sup>†</sup>No 20-kPa Watermark trigger was used in 2004, nor was a nonirrigated conventional treatment used in 2006.

<sup>‡</sup>Irrigation was triggered when any of three sensors buried at depths of 20, 40, and 60 cm reached –40 kPa.

<sup>§</sup>Irrigation was triggered when plots had significantly lower normalized difference vegetation index values than the treatment with the most irrigation applied.

<sup>¶</sup>Irrigation was applied 3 d after aerial trigger unless rainfall occurred.

We propose the use of the green/red ratio for quick, simple estimates of growth and GCF in a production setting. The objectives of this research were to compare visible and NIR aerial imagery-based vegetation indices (Ritchie et al., 2008) and spectrometer ground-based vegetation indices for sensitivity to crop growth, as measured by GCF. The vegetation indices chosen for this study included the green/red ratio, as described by Adamsen et al. (1999), and the red and red-edge variants of the NDVI, as Ritchie and Bednarz (2005) described.

## MATERIALS AND METHODS

### Management

The research was conducted at the Stripling Irrigation Research Park in Camilla, GA during 2004–2006 and was part of a study on remote sensing as a management tool in cotton irrigation. Delta & Pineland 555 BG/RR was seeded in 0.91 m wide rows at a density of 11 plants m<sup>-2</sup> on all planting dates. Planting dates were 5 May 2004, 20 Apr. 2005, and 2 May 2006. Fertility, weed control, insect monitoring and control followed the University of Georgia Cooperative Extension Service Guidelines (Anonymous, 2009). To ensure plant emergence, all plots were irrigated 13 mm before emergence with the overhead system. Crop height was managed using mepiquat chloride at 550 mL ha<sup>-1</sup> at squaring, then 550 to 1400 mL ha<sup>-1</sup> uniformly applied over all treatments at 1 to 2 wk intervals based on management guidelines for a total of 3500 to 4200 mL per year for the studies (Anonymous, 2009).

The irrigation and tillage systems varied by year, due to crop rotation at the irrigation park. The plot layouts, irrigation system, tillage, and irrigation treatments are summarized in Table 1. In 2004, the study was conducted under a variable-rate center pivot based on the design described by Perry et al. (2003). The pivot was programmed to simultaneously apply varying levels of irrigation based on treatment. The treatments were separated by 12 to 20 m of border cotton to allow consistent irrigation within a treatment and prevent overlap with adjacent treatments. All ground-level measurements were made in the center of each treatment to avoid sprinkler overlap. Plot lengths ranged from approximately 21 to 37 m, based on the location of the plot in relationship to the

center pivot. The design was a 4 by 4 Latin square with four irrigation treatments: the well-watered treatment used Watermark (Irrrometer Company, Riverside, CA) sensors placed in each plot at depths of 20, 40, and 60 cm with irrigation triggered at –40 kPa at any depth (40 kPa); an irrigation treatment based on the detection of stress using aerial imagery (Aerial); an irrigation treatment delayed by 3 d from the detection of stress using aerial imagery (Aerial–3 d); and a nonirrigated control.

In 2005 and 2006, the study was conducted on a lateral-move irrigation system designed to allow randomized plot irrigation. The irrigation treatments from 2004 were included, and an additional treatment based on a Watermark trigger of –20 kPa was added (20 kPa trigger). In 2005, all 20 plots were conventional tillage, while in 2006, 20 plots were strip-tilled, randomized with an additional 16 plots that were conventional tillage with the 20 kPa, 40 kPa, Aerial, and Aerial–3 d treatments. As with the 2004 study, overlap between irrigation treatments was minimized by taking measurements in the center of each treatment and separating treatments with border cotton. Plot lengths were 21 m. Early irrigation was applied to all plots after planting at a rate of 13 mm in 2005 and 20 mm in 2006 to ensure uniform emergence.

### Aerial Imagery

Aerial imagery was collected using a two-camera system suspended from a 5-m long and 2.5-m tall tethered blimp (Southern Balloon Works, Deland, FL). The blimp has a 4 kg lift rating by the manufacturer, and was able to carry a 2.5 kg load 250 m high for this study. The camera system consisted of two Nikon 4300 4-megapixel digital cameras (2272 × 1704), one of which was modified to be NIR sensitive (Ritchie et al., 2008), a Digisnap 2100 electronic shutter release device that controlled both cameras (Harbortronics, Gig Harbor, WA), a Schieppati RC switch (KAPshop, Holthees, the Netherlands) that conditioned the electric signal between the remote control radio system and the Digisnap, and a Futaba 4 channel remote control radio system (Tower Hobbies, Champaign, IL) that allowed simultaneous remote firing of the cameras from the ground. The NIR camera was modified by disassembling the camera and replacing the internal hot mirror with a piece of Hoya R72 NIR filter (Hoya Filters, Long Beach, CA) cut to size (Ritchie et al., 2008).

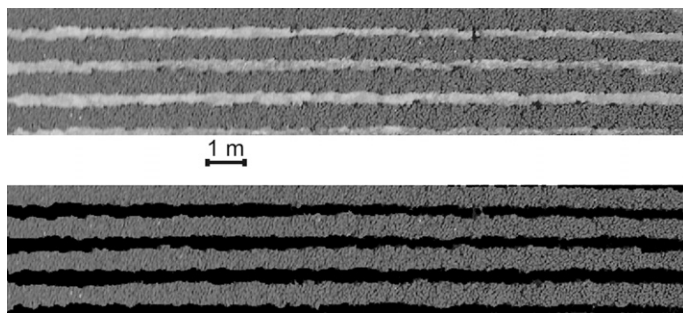


Fig. 1. Ground cover measurements included four plant rows and four soil rows. Plant pixels were separated from soil pixels using the Magic Wand selection tool, as shown by the selection mask in the bottom frame.

The camera settings for each camera were sunlight white balance, ISO 100, no image adjustment, 38-mm focal length (fully zoomed out), and exposure correction applied between visible and NIR cameras. The blimp was flown over the plots at two heights: 45 to 60 m for ground cover measurements, and 180 to 250 m for vegetation index measurements (Ritchie et al., 2008). On some occasions, the ground cover measurement images were collected under cloudy conditions with high ground visibility, but the vegetation index pictures were collected under sunny or partly cloudy conditions to increase the visibility of the blimp for low-flying aircraft and decrease atmospheric variability for the indices. Blimp height was affected somewhat by factors that affected lift and tether angle, including wind and temperature. Blimp height was estimated using marks on the tether strings and verified using the pixel spatial resolution at the center of each image. The blimp was guided by the tethers to each sampling location, and several sample images were taken as the blimp was held above each set of plots to ensure complete plot coverage. Images were collected between 1000 and 1300 h EDT on high visibility days, two to three times per week, with collection dates determined by weather conditions. The blimp platform was quite stable under most weather conditions, and shutter speed rarely decreased below 1/60 s. Consequently, very few images were blurry, and blurry images were excluded from any analyses.

The spectral sensitivity curve of each camera channel was not calculated directly. Instead, the accuracy of the channels in estimating reflectance in broad spectral channels was tested using correlation with the integrated reflectance values of values of colored squares on a GretagMacBeth ColorChecker color panel (X-Rite, Grand Rapids, MI) measured using the spectrometer (Ritchie et al., 2008). The red channel of the visible camera was well-correlated ( $r^2 = 0.98$ ) with integrated reflectance between 600 and 700 nm, and the green channel was well-correlated ( $r^2 = 0.96$ ) with the integrated reflectance between 500 and 600 nm.

The NIR camera blue channel was used for the NIR brightness measurements and was most highly correlated ( $r^2 = 0.99$ ) with reflectance between 800 and 900 nm. The NIR filter in the NIR camera covered the entire imaging array, and all three camera channels were sensitive to NIR radiation. The blue channel of the NIR camera was used as the NIR channel for this research, because it had a high range of sensitivity and did not saturate under high light conditions (Ritchie et al., 2008). Additional information about the spectral sensitivities of the visible and NIR camera channels used in this study, as

well as the modification procedure for the NIR camera, are discussed in detail by Ritchie et al. (2008).

Square (1 m<sup>2</sup>) plywood reflectance panels painted white, gray, and black were placed in the field adjacent to each plot and georeferenced using a Trimble ProXT differential GPS receiver (Trimble Navigation Ltd., Sunnyvale, CA) with sub-meter HRMS accuracy to allow plot identification and image spatial correction. The panels were clearly visible in the images selected for analysis and allowed consistent image alignment. Georeferencing points were made to the northeast corner of each reflectance panel in the image, with a minimum of five alignment points in each image. The reference points were not moved throughout the season, so every image was aligned to the same reference points. In 2004, six to eight rows from each plot were selected for ground cover and vegetation index measurement. In 2005 and 2006, four rows were selected from the center of each plot for image analysis. The visible and NIR images were aligned to the same reference points using the alignment tool in ArcView 3.3 to a root mean square error (RMSE) of <0.1 m throughout each growing season.

## Ground Cover

Ground cover was estimated from the same rows used for vegetation index measurement. Areas of interest included the same number ( $n = 8$  in 2004;  $n = 4$  in 2005–2006) of plant and soil rows (Fig. 1), and were extracted from the images using Adobe Photoshop CS2 (San Jose, CA). Each image was saved in the JPEG image format, which consists of red, green, and blue brightness channels. The quality setting of the camera was set to maximum (least compression), resulting in image files between 1.2 and 1.5 Mb. The brightness channels are viewable and selectable in Adobe Photoshop without any modification to the image.

Image pixels containing plants were spectrally separated from pixels containing soil using the Magic Wand tool, a Photoshop tool that selects spectrally similar pixels in an image. The Magic Wand tool selects pixels throughout the image that are within a user-selected tolerance range of red, green, and blue (RGB) pixel brightness values of a selected pixel. Although the mechanism of the Magic Wand selection tool is proprietary, the algorithm is similar in mode to a three channel parallelepiped classification procedure as described by Mather (2004), which expresses a brightness range in terms of a given number of standard deviation units on either side of the means of selected (RGB) values. Tolerance ranges were usually set between 10 and 15. Soil pixels were selected by hand using the Magic Wand tool and an additive selection procedure that allowed the user to make multiple selections to separate soil pixels from plant pixels. The numbers of plant pixels and total pixels were recorded from the Photoshop histogram values, and GCF was calculated as the ratio of plant pixels to total pixels.

Dark shadows were classified as soil, since the brightness values were low and not spectrally distinct as plants. Classification of shadows has been combined with nonplant image features in more complex rangeland GCF estimates, such as Booth et al. (2006), where the researchers combined the rock and shadow features in images. Due to the GCF images being collected either under cloudy conditions or near solar noon at the relatively south latitude of 31.28° N (Camilla, GA), dark shadows were observed in most cases to constitute <5% of each image.

## Spectrometer Measurements

Ground-level reflectance of each plot was measured using an Apogee VIS-NIR spectrometer (Apogee Instruments, Inc., Logan, UT) with an effective spectral range of 400 to 900 nm and a spectral resolution of 1.4 nm (full width, half maximum height). Each reading consisted of an average of three spectral scans, and two readings were collected per plot on each sampling date. The fiber optic input was held facing nadir to the plant canopy at a height of 1.5 m above the canopy, with a 15° half angle field of view. A white polytetrafluoroethylene (PTFE) reflectance standard was used as a reference, and spectral reflectance by wavelength at each location was calculated as the ratio of plot scene reflectance to the reflectance of the standard, with dark noise subtracted from both the reference and plot measurements. References were collected at 10 to 15 min intervals and after cloud events. Reflectance measurements were collected only when direct sunlight was available, and data collection occurred on average twice a week.

## Camera and Spectrometer Vegetation Indices

Camera NDVI values were calculated from the visible and NIR images using camera brightness values and the relationship between camera brightness, camera exposure, and scene reflectance of the two cameras (Ritchie et al., 2008). The process consisted of calibrating a visible and a NIR camera at multiple exposure levels to a standard reflectance grid under the same lighting conditions to develop a relationship between camera exposure and sensitivity to visible and NIR radiation. The field images were collected simultaneously and corrected for differences in camera exposure, and the corrected images were used for NDVI calculations.

The NDVI for each plot was calculated from the mean image brightness for each plot measured in the visible and NIR channels. The green/red ratio was calculated from the mean green and mean red brightness values from the visible camera for each plot (Adamsen et al., 1999). The purpose of these measurements was to determine whether an index based solely on visible brightness characteristics might be practical for estimation of crop growth.

The red reflectance value used for the spectrometer NDVI ( $NDVI_{spec}$ ) was the average reflectance between 670 and 690 nm, and the NIR reflectance value was the average reflectance between 800 and 840 nm. The red edge reflectance at 710 nm and the NIR average reflectance between 800 and 840 nm were used to calculate the spectrometer red edge NDVI ( $NDVI_{710}$ ). Spectrometer measurements from all treatments were compared with ground cover, with the exception of the most water-stressed treatment on Day 76 after planting in 2004, when significant additional crop wilting was observed between the late morning aerial imagery and the early afternoon spectrometer measurements.

## Analysis

Ground cover measurements using the visible and NIR cameras were evaluated to determine the sensitivity of each system to varying ground cover levels, as well as to determine the relationship between ground cover estimates made using the visible and NIR cameras. The relationship between vegetation indices and ground cover was evaluated using regression analysis ( $\alpha = 0.05$ ), and the error was calculated as the standard error of the estimate. The linear equations were expressed in

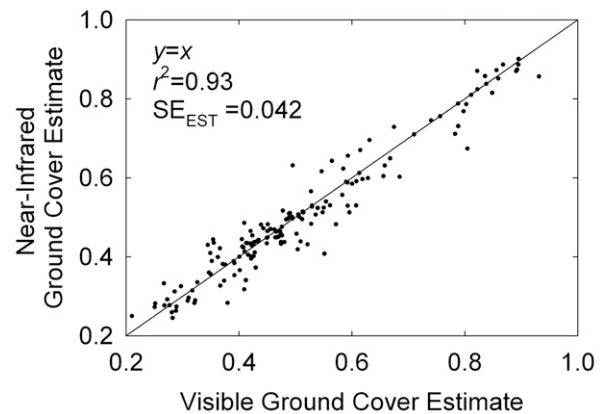


Fig. 2. Comparison of visible and near-infrared ground cover estimates during 2004.

the form  $y = y_0 + ax$ , and higher order equations used  $b$  for the constant of  $x^2$  and  $c$  for the constant of  $x^3$ . Summary statistics of these parameters are included in each graph. Measurements of the GCF via the camera system were compared to (i) camera-derived estimates of vegetation indices, and (ii) spectrometer estimates of vegetation indices measured at ground level. Statistical analysis included both linear and nonlinear regression analysis, determination of the coefficient of variation ( $r^2$ ), and calculation of the standard error of the estimate (SEE).

The camera green/red ratio and NDVI were subsequently compared with GCF measurements over all dates throughout the 3-yr period to determine the ability of the indices to provide estimates of GCF independent of year. The process first tests the significance of the difference of slope between the 3 yr, and then tests the significance of the intercept if the slopes are not significantly different (Clewer and Scarisbrick, 2001). The comparison of the slope by year was performed by producing two regression models. The first model calculated sums of squares based on separate lines that were fit to individual yearly data. The second model calculated sums of squares based on parallel regression lines through the data for each year. The significance of the differences in slope were calculated by the equation:

$$\frac{(\text{ResidSS}_{M2} - \text{ResidSS}_{M3}) / (df_{M2} - df_{M1})}{\text{ResidSS}_{M1} / df_{M1}}$$

on  $(df_{M2} - df_{M1}, df_{M1})$  degrees of freedom, where  $\text{ResidSS}_{M2}$  and  $df_{M2}$  were the residual sum of squares and degrees of freedom of model 2, and  $\text{ResidSS}_{M1}$  and  $df_{M1}$  were the sum of squares and degrees of freedom of model 1. The relationship between years was also tested using ANCOVA (Younger, 1998; Clewer and Scarisbrick, 2001) in SAS 9.1 (The SAS Institute, Cary, NC). In addition, the sensitivity of each index to within-date growth variability was tested by an ANOVA comparison of treatment mean separation ( $\alpha = 0.05$ ) at three crop growth stages: squaring, after first flower, and near peak bloom.

## RESULTS AND DISCUSSION

### Ground Cover Fraction

Ground cover estimates based on visible images were highly correlated with estimates based on NIR images, as shown in Fig. 2 ( $r^2 = 0.93$ ;  $SEE = 0.04$ ). Close relationships were consistently observed between independent

estimates of ground cover, provided the images were taken within 60 m of the crop. As expected, GCF was highly correlated with growth stage: a GCF of 0.20 coincided with growth about 1 wk before first square, and cotton reached a maximum GCF between 0.80 and 1.0 near peak bloom. The highest GCF measurements came from the plots with the highest irrigation levels.

Experimental error related to ground cover estimates appeared to be small, based on comparisons of concurrent GCF estimates from the visible and NIR images (Fig. 2). Much of the experimental error appeared to be due to minor alignment issues, limitations of spatial resolution, and differences in pixel selection based on the tolerance of the Photoshop selection tool. Another potential source of error was the difference in the image characteristics of the visible and NIR cameras. The visible camera has three color channels with which to separate green vegetation from soil. The combination of red, green, and blue channel brightness values is used to separate plants from soil. Only the blue channel of the NIR camera was used, but the high contrast between green vegetation and soil in the NIR simplified plant selection. The relationship between visible and NIR camera ground cover measurements had a similar correlation coefficient to a comparison of independent visible images from the same study. Differences between the visible and NIR camera in measuring GCF were small.

Under favorable conditions, GCF measurements have been shown to be closely related to crop growth and radiation capture (Klassen et al., 2003). Ground cover measurements are most accurate when the image has a high spatial resolution, the plants and soil are spectrally distinct, and shadows do not obscure areas of the image that may be either plant or soil pixels (Booth et al., 2006, 2008; Klassen et al., 2003). The ratio of pixel width to row width (assuming 0.96 m wide rows) was  $1.26 \times 10^{-3}$  of the height of the camera above the canopy. An image collected 50 m from the ground would have 16 pixels across the width of a row of cotton, while an image collected 100 m from the ground would have about eight pixels. In this study, independent images collected at heights <60 m correlated well with each other, while images at heights >60 m above the canopy resulted in increased noise and variability. The difficulties associated with image alignment and image height are more problematic in field plot research with limited space than in a production setting that might cover several rows. The exact relationship between height and spatial resolution depends on both camera optical characteristics and pixel resolution (Dean et al., 2000). The optical system controls the camera focal length, and it can also affect the signal-to-noise ratio at the sensor. Pixel number and spatial resolution are related, since additional pixels sensing a given target area increase the resolution of the image.

The GCF measurements were used as the standard for both camera and spectrometer vegetation indices because of their sensitivity to a broad dynamic range of growth.

However, GCF measurements require imagery with a high spatial resolution, and differentiation between plants and soil can be complicated by shadows, soil texture and brightness, and the difficulty in analyzing pixels that include both soil and plant. The GCF is also time consuming to calculate if done by hand, and computer-based measurements require careful oversight to avoid the effects of changes in lighting, soil background, shadows, and changes in plant reflectance (Hayes and Han, 1993). Nonetheless, this method is appropriate for plot-level measurements of crop growth, since it can measure entire plots at altitudes that allow high spatial resolution. Another advantage is the ability to conduct ground cover measurements on cloudy days, when lighting conditions between one part of a field and another might be different.

### Camera Vegetation Indices

Ground cover estimates were well correlated with vegetation indices throughout the growing season during each year (Table 2). In 2004 and 2006, the spectrometer NDVI<sub>spec</sub> and NDVI<sub>710</sub> had higher Pearson coefficients than the green/red ratio with GCF, but the green/red ratio had a higher Pearson coefficient in 2005. The nonlinearity between the spectrometer green/red ratio and the other spectrometer indices was more pronounced than the nonlinearity between the camera green/red and NDVI indices. There was a high correlation between the camera green/red ratio and the other indices. The camera green/red ratio was linearly correlated ( $r^2 = 0.90$ ) with camera NDVI (Fig. 3) throughout all of the growing seasons. Both of the indices showed similar trends in ground cover across the field throughout each growing season (Fig. 4), and both indices correlated closely with each other when compared on a pixel-by-pixel basis on individual sampling dates (Fig. 5). Although linear regression between camera NDVI and green/red ratio yielded a high  $r^2$  value in a comparison of spectral values throughout a single image, a quadratic equation fit the data better and yielded a higher  $r^2$  (0.94) (Fig. 5). The nonlinearity was observed at low levels of both indices, which corresponded with soil pixels. As shown in Table 2, the green/red ratio correlated more closely with ground cover and spectrometer-based indices than the camera NDVI, although differences in correlation were small.

Part of the errors observed with the camera NDVI may be due to exposure differences and small alignment errors between visible and NIR images. Exposure correction adds a small error to estimates of NDVI, but is unavoidable due to the dramatic difference in plant reflectance between the visible and NIR. Exposure differences between the visible and NIR cameras used for this study ranged from 1/3 to more than 1 1/2 exposure values (f/stops), depending on crop growth (Ritchie et al., 2008).

The study year had an effect on the relationship between both of the camera-based vegetation indices tested and

**Table 2. Season-wide Pearson correlation (*r*) matrices for 2004–2006. All correlations were significant (*P* < 0.05).**

	GCF <sup>†</sup>	NDVI <sub>spec</sub> <sup>‡</sup>	NDVI <sub>710</sub> <sup>§</sup>	Green/red <sub>camera</sub> <sup>¶</sup>	NDVI <sub>camera</sub> <sup>#</sup>	Green/red <sub>spec</sub> <sup>††</sup>
2004GCF	1.00					
NDVI <sub>spec</sub>	0.65	1.00				
NDVI <sub>710</sub>	0.81	0.84	1.00			
Green/red <sub>camera</sub>	0.88	0.85	0.88	1.00		
NDVI <sub>camera</sub>	0.85	0.83	0.86	0.91	1.00	
Green/red <sub>spec</sub> <sup>#</sup>	0.58	0.91	0.54	0.58	0.51	1.00
2005GCF	1.00					
NDVI <sub>spec</sub>	0.64	1.00				
NDVI <sub>710</sub>	0.66	0.85	1.00			
Green/red <sub>camera</sub>	0.94	0.72	0.80	1.00		
NDVI <sub>camera</sub>	0.89	0.70	0.79	0.94	1.00	
Green/red <sub>spec</sub>	0.80	0.80	0.53	0.65	0.67	1.00
2006GCF	1.00					
NDVI <sub>spec</sub>	0.87	1.00				
NDVI <sub>710</sub>	0.89	0.97	1.00			
Green/red <sub>camera</sub>	0.92	0.91	0.93	1.00		
NDVI <sub>camera</sub>	0.91	0.92	0.92	0.96	1.00	
Green/red <sub>spec</sub>	0.59	0.87	0.87	0.81	0.79	1.00

<sup>†</sup>GCF, ground cover fraction

<sup>‡</sup>Spectrometer normalized difference vegetation index.

<sup>§</sup>Spectrometer Red Edge normalized difference vegetation index calculated from R<sub>710 nm</sub> and R<sub>800–840 nm</sub>.

<sup>¶</sup>Camera green/red ratio calculated from visible (VIS) camera green and red channels.

<sup>#</sup>Camera normalized difference vegetation index calculated from near infrared camera blue channel and VIS camera red channel.

<sup>††</sup>Spectrometer green/red ratio calculated from R<sub>550 nm</sub> and R<sub>800–840 nm</sub>.

ground cover. The slopes and intercepts of the relationships between camera vegetation indices and GCF varied across the three growing seasons (2004–2006). The regressions by year between the green/red Ratio and GCF are shown in Fig. 6. The camera green/red ratio and NDVI had very similar relationships to GCF, so the green/red ratio is shown for simplicity. Although the green/red ratio was highly correlated with GCF across the 3-yr period, relationships during these 3 yr had significantly different slopes, based on a comparison of multiple regression lines and ANCOVA (Younger, 1998; Clewer and Scarisbrick, 2001).

Generally, significant differences in slope suggest against pooling data between years or locations. However, as shown in Fig. 6, much of this difference can be attributed to the differences in cotton growth during collection times across the 3 yr. In 2004, vegetative growth was slow, and much of the data was collected at lower GCF than in the 2005 or 2006.

Data collection in 2005 began later in the season due to a tropical weather system that passed through the study site in

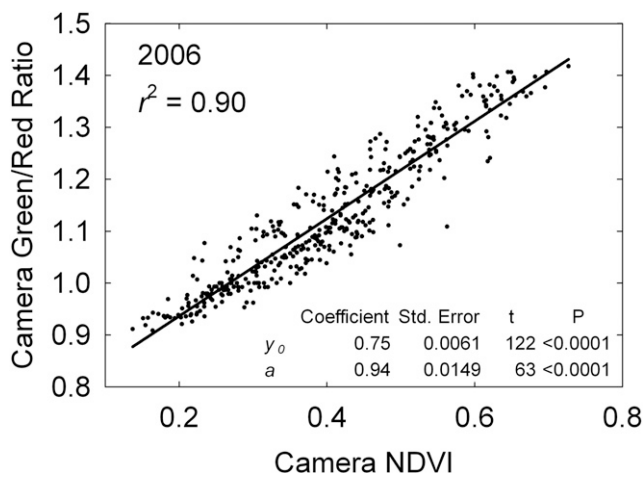


Fig. 3. Comparison of normalized difference vegetation index with camera (NDVI<sub>camera</sub>) green/red ratio for all dates during the 2006 growing season.

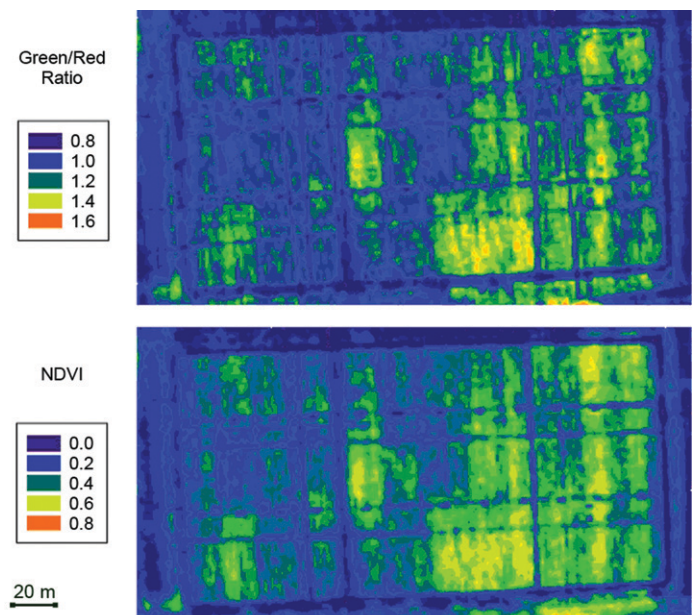


Fig. 4. Green/red ratio and normalized difference vegetation index with camera (NDVI<sub>camera</sub>) on 21 July 2006.

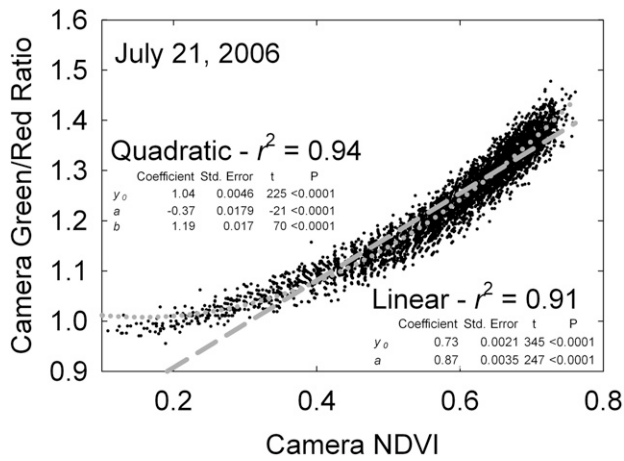


Fig. 5. Relationship of camera green/red ratio with normalized difference vegetation index with camera ( $NDVI_{camera}$ ) on 21 July 2006, calculated from pixel values over the entire field.

late June and early July. The delayed collection, as well as the increased growth due to heavy rainfall throughout the season in 2005, resulted in substantial vegetative growth, and several locations of the field had near maximum ground cover.

In 2006, heavy rainfall periods again resulted in substantial vegetative growth for the irrigation treatments with the highest water application, but GCF measurements were made throughout the season, resulting in a wide range of GCF values. Therefore, the slope of the 2004 relationship was influenced by the comparatively low GCF, and the 2005 slope was influenced by the high GCF. The 2006 regression relationship included both low and high GCF. Spectral indices are limited in dynamic range, an issue that has been reported

by several authors (Carter and Spiering, 2002; Gitelson and Merzlyak, 1997; Horler et al., 1983a). The slopes of the 2005 and 2006 regression lines were not statistically different when measured using the method described by Clewer and Scarisbrick (2001), but the intercept values were significantly different. Combining the 3 yr suggests that the indices are less sensitive to low and high levels of ground cover, but have a strong linear relationship with GCF from 0.20 to 0.80.

The camera green/red ratio was linearly related with camera NDVI throughout the growing season (Fig. 3), even though a ratio index does not have any upper bounding limit, and the NDVI is a normalized ratio with bounding levels of  $-1$  to  $1$ . The linear relationship was due to green and red brightness values being similar in the aerial images. Green/red values ranged from 0.85 to 1.5 between bare soil and complete plant cover. Within such a narrow range of ratios, the relationship between a ratio index and NDVI is mathematically almost completely linear ( $r^2 > 0.99$ ). Therefore, the correlation values obtained using a green/red ratio and a green/red NDVI were virtually identical in this study. The green/red ratio was chosen for emphasis because of its simplicity, as well as the production of negative NDVI values when red brightness values were higher than green brightness values.

### Spectrometer Vegetation Indices

Spectrometer-based spectral indices were closely related with each other. However,  $NDVI_{710}$  showed a greater dynamic range than NDVI (Fig. 7). Both of these indices were more sensitive to GCF than spectrometer green/red ratio, a char-

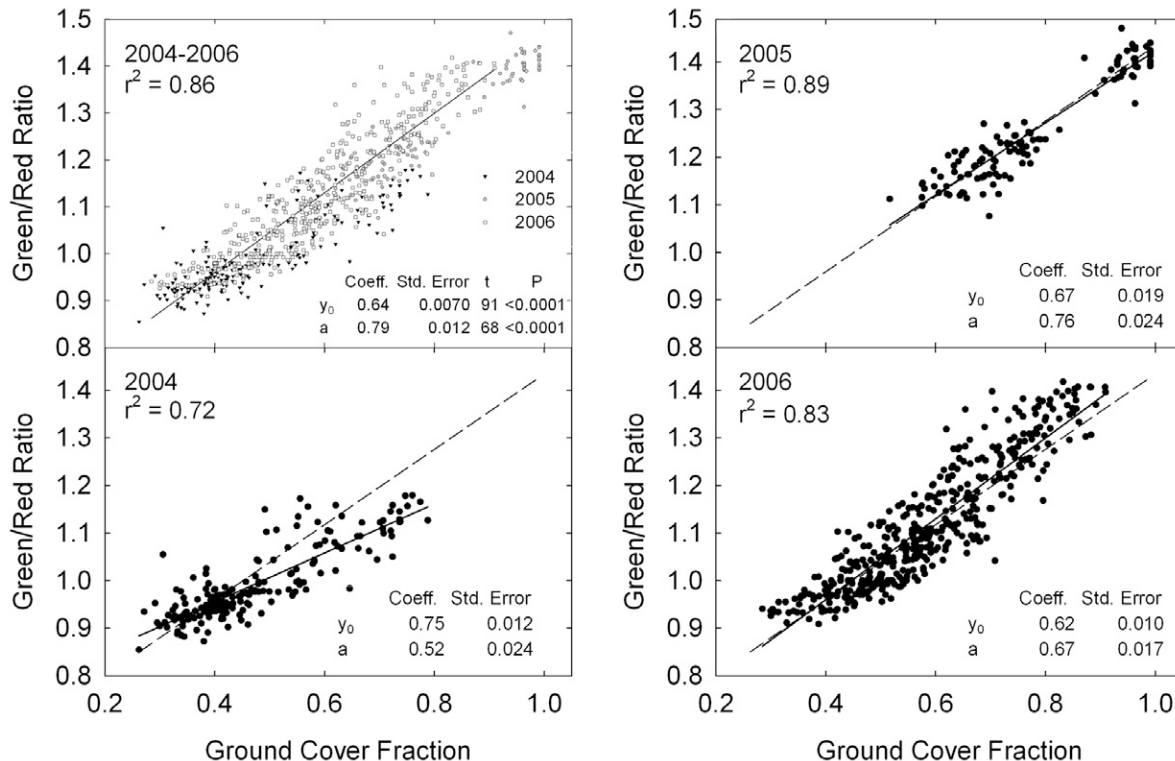


Fig. 6. Relationship between green/red camera ratio and fractional ground cover (2004–2006).

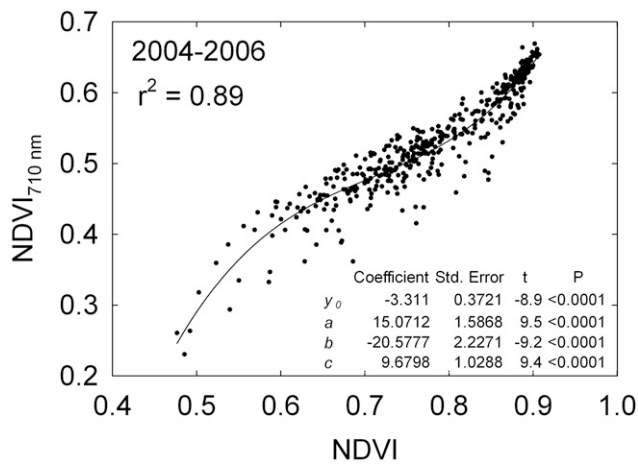


Fig. 7. Comparison of spectrometer normalized difference vegetation index calculated from  $R_{710\text{nm}}$  ( $\text{NDVI}_{710\text{nm}}$ ) with spectrometer NDVI (2004–2006).

acteristic that agrees with other studies on ground-based reflectance indices in cotton (Ritchie and Bednarz, 2005).

The  $\text{NDVI}_{710}$  index reached a maximum at a GCF of <0.80 (Fig. 8). This index also reached a maximum at camera green/red ratio values >1.3 (Fig. 9). These findings suggest that spectrometer  $\text{NDVI}_{710}$  is less sensitive to high levels of ground cover than is the camera green/red ratio. However, Fig. 9 also indicates that  $\text{NDVI}_{710}$  is more sensitive to low levels of ground cover than the camera green/red ratio.

None of the spectral indices were sensitive to a full range of GCF. The  $\text{NDVI}_{710}$  was more sensitive to low levels of vegetation than the camera indices (Fig. 9), but was less sensitive to high GFC. Some of the decreased sensitivity of the spectrometer indices to high GCF may be due to the influence of plant height on the sensor field of view. Klassen et al. (2003) emphasized that in close-proximity measurements, the increased influence of the plant material causes an overestimation of plant size, since the plants are nearer than the soil to the sensor. This overestimated green cover, in turn, would result in saturation of the vegetation index at a lower level than if the spectrometer was further from the plants.

The spectrometer  $\text{NDVI}_{710}$  had better dynamic range than spectrometer NDVI, as well as a higher correlation with ground cover and camera vegetation indexes. This agrees with other studies (Carter and Spiering, 2002; Horler et al., 1983a, 1983b; Ritchie and Bednarz, 2005) that suggest that red edge measurements can improve the dynamic range of indices used to estimate chlorophyll density at both the leaf and plant canopy levels.

An observed source of error in the relationship between camera and spectrometer estimates of NDVI was the difference in coverage area between the two systems. Spectrometer and camera NDVI values of individual plots were highly correlated, particularly in the well-watered treatments (data not shown), with  $r^2$  values ranging from 0.66 to 0.96 in the strip tillage plots, and from 0.78 to 0.95 in the conventional tillage plots. However, the slopes of the

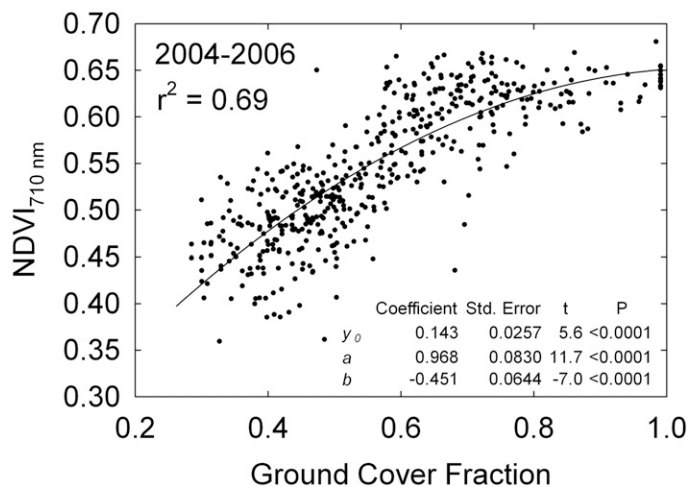


Fig. 8. Comparison of spectrometer normalized difference vegetation index calculated from  $R_{710\text{nm}}$  ( $\text{NDVI}_{710}$ ) with GCF (2004–2006).

regression lines for individual plots differed significantly, due to variability in the growth between the sampling location for the spectrometer and the entire plot sampled by the camera images. The plots with the lowest coefficients of determination were the treatments with the most water stress, where growth within a plot varied more.

## Treatment Comparisons

A comparison of indices during 2006 at squaring, early bloom, and near peak bloom is shown in Table 3. All of the indices showed significant differences at the  $P = 0.05$  level between irrigation treatments at all three dates, with the exception of the camera NDVI index ( $P = 0.075$ ). In addition, mean comparisons using camera NDVI had higher treatment variances and lower significance levels at all dates than the other comparisons. At least part of this variance can be attributed to differences in exposure

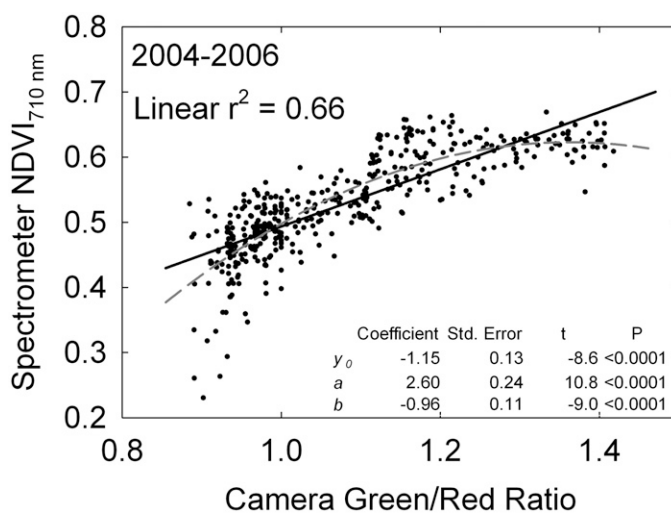


Fig. 9. Relationship of normalized difference vegetation index calculated from  $R_{710\text{nm}}$  ( $\text{NDVI}_{710}$ ) collected with the spectrometer with the green/red ratio collected with the visible camera (2004–2006).

**Table 3. Vegetation index and ground cover fraction (GCF) treatment means by irrigation at three crop growth stages (2006).**

Crop stage		20-cbar	40-cbar	Aerial	Aerial-3 d	Nonirrigated	LSD (0.05)
Early square	GCF	0.528 ± 0.007 a <sup>†</sup>	0.479 ± 0.017 b	0.445 ± 0.022 b	0.459 ± 0.020 b	0.468 ± 0.012 b	0.045
	Green/red	1.030 ± 0.039 ab	1.029 ± 0.022 ab	1.044 ± 0.025 a	0.977 ± 0.010 b	0.985 ± 0.009 b	0.059
	NDVI <sub>710</sub> <sup>‡</sup>	0.488 ± 0.011 a	0.503 ± 0.005 a	0.486 ± 0.017 ab	0.510 ± 0.010 a	0.467 ± 0.022 b	0.027
	NDVI <sub>spec</sub> <sup>§</sup>	0.339 ± 0.030 a	0.354 ± 0.024 a	0.341 ± 0.021 a	0.298 ± 0.004 a	0.293 ± 0.006 b	0.041
	NDVI <sub>camera</sub> <sup>¶</sup>	0.780 ± 0.014 ab	0.775 ± 0.013 a	0.777 ± 0.011 ab	0.785 ± 0.006 b	0.718 ± 0.023 b	0.054
Early bloom	GCF	0.532 ± 0.012 a	0.505 ± 0.036 ab	0.531 ± 0.022 a	0.496 ± 0.021 ab	0.459 ± 0.015 b	0.067
	Green/red	1.071 ± 0.038 a	1.047 ± 0.029 ab	1.058 ± 0.043 a	1.013 ± 0.012 b	1.004 ± 0.013 b	0.079
	NDVI <sub>710</sub>	0.520 ± 0.016 a	0.524 ± 0.011 a	0.524 ± 0.013 a	0.534 ± 0.005 a	0.489 ± 0.014 b	0.020
	NDVI <sub>spec</sub>	0.391 ± 0.046 a	0.350 ± 0.034 a	0.369 ± 0.063 a	0.327 ± 0.027 a	0.299 ± 0.047 b	0.026
	NDVI <sub>camera</sub>	0.718 ± 0.012	0.745 ± 0.009	0.724 ± 0.016	0.705 ± 0.013	0.647 ± 0.039	ns <sup>#</sup>
Peak bloom	GCF	0.736 ± 0.061 a	0.745 ± 0.049 a	0.780 ± 0.052 a	0.695 ± 0.026 ab	0.602 ± 0.052 b	0.110
	Green/red	1.275 ± 0.044 a	1.308 ± 0.044 a	1.305 ± 0.049 a	1.245 ± 0.025 ab	1.182 ± 0.041 b	0.079
	NDVI <sub>710</sub>	0.616 ± 0.010 a	0.621 ± 0.009 a	0.626 ± 0.010 a	0.624 ± 0.004 ab	0.587 ± 0.008 b	0.022
	NDVI <sub>spec</sub>	0.564 ± 0.042 a	0.570 ± 0.045 a	0.563 ± 0.048 a	0.530 ± 0.027 ab	0.469 ± 0.060 b	0.026
	NDVI <sub>camera</sub>	0.880 ± 0.009 a	0.888 ± 0.004 a	0.879 ± 0.011 a	0.882 ± 0.002 ab	0.846 ± 0.009 b	0.074

<sup>†</sup>Horizontal means with the same letter are not significantly different ( $\alpha = 0.05$ ).

<sup>‡</sup>Spectrometer Red Edge normalized difference vegetation index calculated from  $R_{710\text{ nm}}$  and  $R_{800-840\text{ nm}}$ .

<sup>§</sup>Spectrometer normalized difference vegetation index.

<sup>¶</sup>Camera normalized difference vegetation index calculated from near infrared camera blue channel and VIS camera red channel.

<sup>#</sup>Not significant.

settings and minor alignment issues between the cameras that have been previously discussed.

## CONCLUSIONS

The results from this study suggest that the camera NDVI, camera green/red ratio, and spectrometer NDVI<sub>710 nm</sub> indices all have useful attributes for specific remote sensing needs and can estimate GCF between 0.20 and 0.80. The higher sensitivity of the spectrometer NDVI<sub>710 nm</sub> compared to the spectrometer NDVI suggests that NDVI<sub>710 nm</sub> would be more appropriate for ground-based measurement systems. However, aerial systems based on this index would require more extensive consumer camera modification than indices based on visible channels. The consistency of the aerial NDVI measurements over the growing season, despite the wide range of camera exposure differences between the visible and NIR cameras, suggests that this index can provide a robust NDVI estimate.

The green/red ratio, which has already been shown to be effective for estimating leaf senescence (Adamsen et al., 1999), also provides a very simple method for ground cover estimates, although it may be less sensitive to low levels of ground cover than the NDVI. Another advantage of the green/red ratio is the ability to use a single digital camera to collect both channels, so it is not necessary to align images from different cameras in software. These characteristics make the green/red ratio useful as a simple, low-cost, single camera system for remote sensing of crop growth. The high linear correlation between the green/red ratio and GCF measurements over a 3-yr period suggests that this index can provide a robust estimate of crop growth, despite its simplicity. The value of the green/red ratio is that those with limited experience, technical capabilities, or resources

have access to technology that is quick, accurate, and easy to apply in a crop production setting.

## References

- Adamsen, F., P. Pinter, E. Barnes, R. LaMorte, G. Wall, S. Leavitt, and B. Kimball. 1999. Measuring wheat senescence with a digital camera. *Crop Sci.* 39:719–724.
- Anonymous. 2009. 2009 Georgia cotton production guide, Vol. ENT-09-01. The Univ. of Georgia College of Agric. and Environ. Sci., Athens.
- ASD. 1999. Technical guide, 3rd ed. Analytical Spectral Devices, Inc., Boulder, CO.
- Asrar, G., R.B. Myneni, and B.J. Choudhury. 1992. Spatial heterogeneity in vegetation canopies and remote sensing of absorbed photosynthetically active radiation: A modeling study. *Remote Sens. Environ.* 41:85–103.
- Bannari, A., D. Morin, F. Bonn, and A.R. Huete. 1995. A review of vegetation indices. *Remote Sens. Rev.* 13:95–120.
- Boissard, P., J.-G. Pointel, and J. Tranchefort. 1992. Estimation of the ground cover ratio of a wheat canopy using radiometry. *Int. J. Remote Sens.* 13:1681–1692.
- Booth, D.T., S.E. Cox, T.W. Meikle, and C. Fitzgerald. 2006. The accuracy of ground-cover measurements. *Rangeland Ecol. Manage.* 59:179–188.
- Booth, D.T., S.E. Cox, T. Meikle, and R.R. Zuuring. 2008. Ground-cover measurements: Assessing correlation among aerial and ground-based methods. *Environ. Manage.* 42:1091–1100.
- Broge, N.H., and E. Leblanc. 2001. Comparing prediction power and stability of broadband and hyperspectral vegetation indices for estimation of green leaf area index and canopy chlorophyll density. *Remote Sens. Environ.* 76:156–172.
- Calera, A., C. Martínez, and J. Melia. 2001. A procedure for obtaining green plant cover: Relation to NDVI in a case study for barley. *Int. J. Remote Sens.* 22:3357–3362.
- Carter, G.A., and B.A. Spiering. 2002. Optical properties of intact leave for estimating chlorophyll concentration. *J. Environ. Qual.* 31:1424–1432.

- Chen, X., and L. Vierling. 2006. Spectral mixture analyses of hyperspectral data acquired using a tethered balloon. *Remote Sens. Environ.* 103:338–350.
- Clewer, A.G., and D.H. Scarisbrick. 2001. *Practical statistics and experimental design for plant and crop science*. John Wiley & Sons, Chichester, England.
- Curran, P.J. 1989. Remote sensing of foliar chemistry. *Remote Sens. Environ.* 30:271–278.
- Dean, C., T.A. Warner, and J.B. McGraw. 2000. Suitability of the DCS460c colour digital camera for quantitative remote sensing analysis of vegetation. *ISPRS J. Photogram. Remote Sens.* 55:105–118.
- Elvidge, C.D., and Z. Chen. 1995. Comparison of broad-band and narrow-band red and near-infrared vegetation indices. *Remote Sens. Environ.* 54:38–48.
- Gitelson, A.A., and M.N. Merzlyak. 1997. Remote estimation of chlorophyll content in higher plant leaves. *Int. J. Remote Sens.* 18:2691–2697.
- Gitelson, A.A., and M.N. Merzlyak. 1998. Remote sensing of chlorophyll concentration in higher plant leaves. *Adv. Space Res.* 22:689–692.
- Hatfield, J.L., A.A. Gitelson, J.S. Shepers, and C.L. Walthall. 2008. Application of spectral remote sensing for agronomic decisions. *Agron. J.* 100:S-117–130.
- Hayes, J.C., and Y.J. Han. 1993. Comparison of crop-cover measuring systems. *Trans. ASAE* 36:1727–1732.
- Horler, D.N.H., M. Dockray, and J. Barber. 1983a. The red edge of plant leaf reflectance. *Int. J. Remote Sens.* 4:273–288.
- Horler, D.N.H., M. Dockray, J. Barber, and A.R. Barringer. 1983b. Red edge measurements for remotely sensing plant chlorophyll content. *Adv. Space Res.* 3:273–277.
- Huete, A.R. 1988. A soil-adjusted vegetation index (SAVI). *Remote Sens. Environ.* 25:295–309.
- Huete, A.R., R.D. Jackson, and D.F. Post. 1985. Spectral response of a plant canopy with different soil backgrounds. *Remote Sens. Environ.* 17:37–53.
- Kanemasu, E.T. 1974. Seasonal canopy reflectance patterns of wheat, sorghum, and soybean. *Remote Sens. Environ.* 3:43–47.
- Klassen, S.P., G. Ritchie, J. Frantz, D. Pinnock, and B. Bugbee. 2003. Real-time imaging of ground cover: Relationships with radiation capture, canopy photosynthesis, and daily growth rate. p. 3–14. *In* T. VanToai et al. (ed.) *Digital imaging and spectral techniques: Applications to precision agriculture and crop physiology* ASA Spec. Publ. 66. ASA, CSSA, and SSSA, Madison, WI.
- Mather, P.M. 2004. *Computer processing of remotely-sensed images: An introduction*. 3rd ed. John Wiley & Sons, Hoboken, NJ.
- Osborne, S.L., J.S. Schepers, D.D. Francis, and M.R. Schlemmer. 2002. Use of spectral radiance to estimate in-season biomass and grain yield in nitrogen- and water-stressed corn. *Crop Sci.* 42:165–171.
- Perry, C.D., S. Pocknee, and O. Hansen. 2003. A variable rate pivot irrigation control system. p. 539–544. *In* J.V. Stafford and A. Werner (ed.) *Proc. of the 4th European Conf. on Precision Agric. (4ECPA)*, Berlin, Germany. May 2003. Wageningen Academic Publishers, Wageningen, the Netherlands.
- Pinter, P.J., J.L. Hatfield, J.S. Schepers, E.M. Barnes, M.S. Moran, C.S.T. Daughtry, and D.R. Upchurch. 2003. Remote sensing for crop management. *Photogram. Eng. Remote Sens.* 69:647–664.
- Plant, R.E., D.S. Munk, B.R. Roberts, R.L. Vargas, D.W. Rains, R.L. Travis, and R.B. Huttmacher. 2000. Relationships between remotely sensed reflectance data and cotton growth and yield. *Trans. ASAE* 43:535–546.
- Purevdorj, T., R. Tateishi, T. Ishiyama, and Y. Honda. 1998. Relationships between percent vegetation cover and vegetation indices. *Int. J. Remote Sens.* 19:3519–3535.
- Ritchie, G.L., and C.W. Bednarz. 2005. Estimating defoliation of two distinct cotton types using reflectance data. *J. Cotton Sci.* 9:182–188.
- Ritchie, G.L., D.G. Sullivan, C.D. Perry, J.W. Hook, and C.W. Bednarz. 2008. Preparation of a low-cost digital camera system for remote sensing. *Appl. Eng. Agric.* 24:885–894.
- Rouse, J.W., R.H. Haas, J.A. Schell, and D.W. Deering. 1973. Monitoring vegetation systems in the great plains with ERTS. p. 309–317. *Third Earth Resources Technol. Satellite-1 Symp.*, NASA SP-351, Vol. 1. NASA, Washington, DC.
- Sui, R., J.B. Wilkerson, W.E. Hart, L.R. Wilhelm, and D.D. Howard. 2005. Multi-spectral sensor for detection of nitrogen status in cotton. *Appl. Eng. Agric.* 21:167–172.
- Thenkabail, P.S., R.B. Smith, and E.D. Pauw. 2002. Evaluation of narrowband and broadband vegetation indices for determining optimal hyperspectral wavebands for agricultural crop characterization. *Photogram. Eng. Remote Sens.* 68:607–621.
- Tucker, C.J. 1979. Red and photographic infrared linear combinations for monitoring vegetation. *Remote Sens. Environ.* 8:127–150.
- Vierling, L., M. Fersdahl, X. Chen, Z. Li, and P. Zimmerman. 2006. The short-wave aerostat-mounted imager (SWAMI): A novel platform for acquiring remotely sensed data from a tethered balloon. *Remote Sens. Environ.* 103:255–264.
- Yang, C., J.M. Bradford, and C.L. Wiegand. 2001. Airborne multispectral imagery for mapping variable growing conditions and yields of cotton, grain sorghum, and corn. *Trans. ASAE* 44:1983–1994.
- Yang, C., S.M. Greenberg, J.H. Everitt, T.W. Sappington, and J.J.W. Norman. 2003. Evaluation of cotton defoliation strategies using airborne multispectral imagery. *Trans. ASAE* 46:869–876.
- Younger, M.S. 1998. *Statistical research methods in the life sciences*. Duxbury Press, Belmont, CA.